Geometric Control using Geodesics and Parallel Transport

by

Byunghoon Kim

Master of Science Thesis

Department of Mechanical and Aerospace Engineering

SEOUL NATIONAL UNIVERSITY

August 2013

Abstract

Geometric Control using Geodesics and Parallel Transport

Byunghoon Kim
Department of Mechanical and Aerospace Engineering
The Graduate School
Seoul National University

In this thesis, a novel geometric tracking controller for a fully actuated rigid body system is proposed utilizing the geodesic distance and the parallel transport along the geodesic. The choice of geodesic distance allows us to design a position error vector which is exactly proportional to the actual size of the error. A geometric controller based on the previous choice is investigated, especially for the case of $SO(3)$. Numerical simulation is carried out using the state-of-the-art Lie group integrator which preserves Lie group structure so that produces a very accurate results. Simulation results are compared among three different choice of configuration error function.

Keyword: Geometric Control, Lyapunov Control, Geodesics, Parallel Transport
Student Number: 2011-23327

Contents

List of Figures

Chapter 1

Introduction

Acrobatic maneuver of a rotorcraft requires a highly robust and very fast controller that can handle sudden change of large position error as well as large velocity error. Apparent disadvantages are observed in case of the local coordinate representation based approach, such as using Euler angles or quarternions, because some problems are merely induced by the choice of a coordinate and are not inherent problems of the given situation. [7]

Many authors actively investigated the geometric control which is to design a stabilizer of tracking controller directly on the configuration manifold avoiding the arbitrary choice of any coordinate system.[1, 12]

Some authors[4] show very thorough and systematic approach based on the differential geometry and Lie group theory. A general Lyapunov based geometric controller is proposed on the condition that one can find a compatible pair of a configuration error on the given manifold and the transport map of the tangent vectors. If such pair can be found, it is shown that stabilizes exponentially or that tracks the reference trajectory asymtotically. However, they showed some examples of possible compatible pairs.

We start to think about the choice of these pairs with the geodesic distance of the given manifold of Lie group and the parallel transport along it. Trivial $\mathbb{R}^3$ case and important $SO(3)$ case will be investigated.

Chapter 2

Mathematical Preliminaries

In this chapter, we briefly review some mathematical concepts that are essential in the following chapters. For more detailed exposition of Riemannian Geometry, we refer to [2, 6]. For an introduction to Lie group, we refer to [14, 8].

2.1 Riemannian Geometry

A smooth manifold M with a Riemannian metric $\mathbb{G}$ defined on it is said to be a *Riemannian manifold* $(M, \mathbb{G})$. A C^k-*Riemannian metric* on M is a class $C^k(0,2)$-tensor field $\mathbb{G}$ on M

$$\mathbb{G}(x) : T_xM \times T_xM \to \mathbb{R}$$

having the property that $\mathbb{G}(x)$ is an inner product on T_xM. For $x \in M$, we have associated isomorphisms

$$\mathbb{G}^\flat(x) : T_xM \to T_x^*M$$
$$\mathbb{G}^\sharp(x) : T_x^*M \to T_xM,$$

and the inner product of covectors on T_x^*M

$$\mathbb{G}^{-1}(x) : T_x^*M \times T_x^*M \to \mathbb{R}$$

is defined by

$$\mathbb{G}^{-1}(\alpha_x, \beta_x) := \mathbb{G}(\mathbb{G}^\sharp(\alpha_x), \mathbb{G}^\sharp(\beta_x)).$$

An *affine connection* ∇ on M is a smooth map that assigns to the pair (X, Y) of smooth vector fields X and Y a vector field $\nabla_X Y$ such that the following properties are satisfied:

(i) $(X, Y) \mapsto \nabla_X Y$ is $\mathbb{R}$-bilinear,

(ii) $\nabla_{fX} Y = f \nabla_X Y$ for all function f on M,

(iii) $\nabla_X fY = f \nabla_X Y + (\mathcal{L}_X f) Y$ for all function f on M, where $\mathcal{L}_X f$ is the Lie derivative of f.

Using the *Christoffel symbols* Γ^k_{ij} for an affine connection, the coordinate formula for the *covariant derivative* of Y with respect to X is

$$\nabla_X Y = (\frac{\partial Y^k}{\partial x^i} X^i + \Gamma^k_{ij} X^i Y^j) \frac{\partial}{\partial x^k}. \tag{2.1}$$

A certain affine connection is of more interest. The *Levi-Civita affine connection* $\overset{\mathbb{G}}{\nabla}$ is an affine connection uniquely determined by a given Riemmanian metric $\mathbb{G}$ such that

(i) $\overset{\mathbb{G}}{\nabla}$ is a metric connection, or $\nabla \mathbb{G} = 0$,

(ii) $\overset{\mathbb{G}}{\nabla}_X Y - \overset{\mathbb{G}}{\nabla}_Y X = [X, Y]$ for all vector fields $X, Y \in TM$.

2.2 Lie Group

A *Lie group* $(G, \star)$ is a topological group that is also a manifold, in which the group and the inverse operations are smooth. A *Lie algebra* $\mathfrak{g}$ is $\mathbb{R}$-vector space endowed with a bilinear operation $[\cdot, \cdot]$.

The group structure of a Lie group induces the *left translation map* such that

$$\begin{aligned} L_g : G &\to G \\ h &\mapsto g \star h, \end{aligned}$$

and for $g \in G$, the natural isomorphism between tangent spaces is given by $T_e L_g : T_e G \to T_g G$. The *right translation map* $R_g : G \to G$ and its tangent map $T_e R_g : T_e G \to T_g G$ are also defined in the similar manner.

From the left translation map, we define the *left-invariant vector field*, a *left-invariant Riemannian metric*, and a *left-invariant affine connection*.

A vector field is left-invariant if $L_g^* X(h) = X(L_g h)$ is equal to $T_h L_g(X(h))$.

A left-invariant Riemmanian metric $\mathbb{G}$ on a Lie group $(G, \star)$ satisfies

$$\mathbb{G}(g) \cdot (X_g, Y_g) = \mathbb{G}(h \star g) \cdot (T_g L_h(X_g), T_g L_h(Y_g)).$$

Moreover, if we define an inner product $\mathbb{I}$ on $\mathfrak{g}$ a smooth left-invarint Riemanian metric $\mathbb{G}_{\mathbb{I}}$ on G can be expressed in terms of the inner product $\mathbb{I}$ on $\mathfrak{g}$ as follows:

$$\mathbb{G}_{\mathbb{I}}(g) \cdot (X_g, Y_g) = \mathbb{I}(T_g L_{g^{-1}}(X_g), T_g L_{g^{-1}}(Y_g)).$$

A left-invariant affine connection on G satisfies $L_g^*(\nabla_X Y) = \nabla_{L_g^* X} L_g^* Y$.

Similarly, the right tranlation map gives the right-invariant vector field, a right-invariant Riemannian metric and a right-invariant affine connection. Finally, if a Riemannian metric is both left- and right-invariant, it is called *bi-invariant* Riemannian metric; if an affine connection is as such, it is called a *bi-invariant* affine connection.

An *exponential map* is a map from the given Lie algebra $\mathfrak{g}$ to its associated Lie group G such that

$$\begin{aligned} exp : \mathfrak{g} &\to G \\ \xi &\mapsto exp(\xi) = \Phi_1^{\xi_L}(e), \end{aligned}$$

where ξ_L is the left-invariant vector field whose value is ξ at the identity elemnt e of G and $\Phi_1^{\xi_L}(e)$ is the flow from the identity element e of G along the vector field ξ_L. The image of a smoothe group homomorphism $\rho : \mathbb{R} \to G$ is the integral curve $\rho(t) = exp(t\xi) = \Phi_t^{\xi_L}(e)$ called a *one-parameter subgroup* of G.

2.3 Geodesics and Parallel Transport

If an affine connection is defined, two important definitions naturally follow; geodesics and the parallel transport.

2.3.1 Geodesics and Parallel Transport on a Riemannian Manifold

A *geodesic* of an affine connection, especially of a Levi-Civita affine coonection for our use, on M is a curve $\gamma : I \mapsto M$ satisfyling

$$\overset{\mathbb{G}}{\nabla}_{\gamma'(t)}\gamma'(t) = 0. \tag{2.2}$$

The *parallel transport* is the map $\tau_{t_0,t}^{\gamma} : T_{\gamma(t_0)}M \mapsto T_{\gamma(t)}M$ that moves a vector $X(t_0) \in T_{\gamma(t_0)}M$ to the vector $X(t) \in T_{\gamma(t)}M$ in a parallel way. Given a curve $\gamma(t) \in M$, a vector field $X(t) \in T_{\gamma(t)}$ is said to be *parallel* if

$$\overset{\mathbb{G}}{\nabla}_{\gamma'(t)}X(t) = 0. \tag{2.3}$$

For example, on a Riemannian manifold $(\mathbb{R}^3, \mathbb{G})$ the geodesic equation (2.2) can be written in coordinates according to (2.1) as

$$\ddot{\gamma} = 0, \qquad \gamma \in \mathbb{R}^3.$$

The solution to this second order differential equation with the boundary condition $\gamma(t_0) = x_0$ and $\gamma(t_f) = x_f \in \mathbb{R}^3$ is simply a straight line connecting x_0 and x_f.

The parallel transport equation (2.3) along a geodesic $\gamma(t)$ can be written in coordinates as

$$\begin{aligned} \dot{X}^i(t) &= 0 \qquad \text{where} \quad i \in \{1, 2, 3\} \\ X^i(0) &= X_0^i. \end{aligned}$$

The solution to the systems of first order differential equations is a constant vector field on $\mathbb{R}^3$.

2.3.2 Geodesic and Parallel Transport on a Lie Group

To obtain the geodeics on a general Riemannian manifold, we often have to solve the system of the second order differential equations with non-constant coeffients, which is not at all an easy task. After solved for the geodesic, to get the parallel transport requires to solve another system of the first order differential equations.

However, this can be greatly simplified if we know the given Riemannian manifold is actually a symmetric one. For example, every compact connected Lie group G can be proved to be a symmetric space with respect to the bi-invariant metric. Moreover, a geodesic connecting any two points on a compact, connected Lie group G with bi-invariant metric is either the one-parameter subgroup or the left(or right) translation of these one-parameter subgroups.[2]

If G is the special orthogonal group $SO(3)$, then the bi-invariant metric is always defined by the Frobenious inner product of its Lie algebra $so(3)$ as

$$\begin{aligned} \mathbb{G}(g) \cdot (X(g), Y(g)) &= \mathbb{G}(e) \cdot (T_g L_{g^{-1}} X(g), T_g L_{g^{-1}} Y(g)) \\ &= \mathbb{G}(e) \cdot (X(e), Y(e)) \\ &:= trace(Y(e)^T X(e)). \end{aligned}$$

It is trivial to show Riemannian metric defined as above is bi-invariant.

Hence, the geodesic connecting g and $g_{ref} \in SO(3)$ is obtained without solving any differential equation.

$$\gamma(t) = g_{ref} exp(t\xi) \qquad \text{where} \quad \xi = log(g_{ref}^T g). \tag{2.4}$$

The parallel transport of a tangent vector $\tau^{\gamma}_{g_{ref},g} : T_{g_{ref}} \to T_g$ is shown to be

$$\tau^{\gamma}_{g_{ref},g}(\dot{g_{ref}}) = TL(exp(\frac{\xi}{2}))TR(exp(\frac{\xi}{2}))TL_{g_{ref}^{-1}}(\dot{g_{ref}}). \tag{2.5}$$

If the bi-invariant metric cannot be defined on a Lie group G but the defined Riemannian affine connection is either $+$ or $-$ Cartan-Schouten connections, the geodesic and the one-parameter subgroup on G still coincides and the parallel transport in these cases become[8]

$$\tau^{\gamma}_{g_{ref},g}(\dot{g_{ref}}) = TL_{g_{ref}^{-1}g}(\dot{g_{ref}}), \qquad \text{if left(or +)-Cartan} \tag{2.6}$$

$$\tau^{\gamma}_{g_{ref},g}(\dot{g_{ref}}) = TR_{g_{ref}^{-1}g}(\dot{g_{ref}}). \qquad \text{if right(or -)-Cartan.} \tag{2.7}$$

Matrix exponetial is defined as

$$\exp A = \sum_{k=0}^{+\infty} \frac{A^k}{k!}.$$

Especially for $SO(3)$, matrix exponential can be written as

$$\exp \hat{\omega} = \begin{cases} I_3 & \omega = 0, \\ I_3 + \frac{\sin\|\omega\|_{\mathbb{R}^3}}{\|\omega\|_{\mathbb{R}^3}}\hat{\omega} + \frac{1-cos\|\omega\|_{\mathbb{R}^3}}{\|\omega\|_{\mathbb{R}^3}}\hat{\omega}^2 & \omega \neq 0 \end{cases} \tag{2.8}$$

where $\omega \in \mathbb{R}^3$, and $\cdot^{\vee} : \mathfrak{so}(3) \to \mathbb{R}^3$ is the inverse map of $\cdot^{\wedge} : \mathbb{R}^3 \to \mathfrak{so}(3)$ by $\hat{\omega} y = \omega \times y$ for all $\omega, y \in \mathbb{R}^3$. Equation (2.8) is referred to as *Rodrigues's Formula.*

Matrix logarithm is define as the inverse map of the matrix exponential.

$$log : \{R \in SO(3) | trace(R) \neq -1\} \to \{\hat{\omega} \in \mathfrak{so}(3) | \omega \in \mathbb{R}^3, \quad \| \omega \|_{\mathbb{R}^3} < \pi\}$$

is given by[4]

$$log(R) = \begin{cases} 0_3 & R = I_3, \\ \frac{\phi(R)}{2\sin(\phi(R))}(R - R^T) & R \neq I_3, \end{cases}$$
$$\text{where} \quad \phi(R) = \arccos(\frac{1}{2}(tr(R) - 1)).$$

Chapter 3

Geometric control using Geodesics and Parallel Transport

In this chapter, we quickly review equations of motion on a general Riemannian manifold $(M, \mathbb{G})$ and on a connected compact Lie group $(G, \star)$. Especially, the cases of $\mathbb{R}^3$ and $SO(3)$ are considered, respectively. Then, we follow the argument of [4] to design a geometric tracking controller for each case. A novel pair of error function and transport map $(\Psi, \mathcal{T})$ using the geodesic distance and the parallel transport is proposed to design the geometric tracking controller.

3.1 Equations of Motion

Applying the Lagrange-d'Alembert Principle on Riemannian manifolds to a fully actuated C^∞-simple mechanical control system $\Sigma = (M, \mathbb{G}, V = 0, \mathcal{F})$, where $\mathbb{G}$ is a Riemannian metric which is equal to the twice of the system's kinetic energy, V is a potential field and $\mathcal{F}$ is a collection of allowed control forces, the equations of motion along a trajectory $\gamma(t) \in M$ becomes

$$\overset{\mathbb{G}}{\nabla}_{\gamma'(t)}\gamma'(t) = \mathbb{G}^\sharp(F(t, \gamma'(t))). \tag{3.1}$$

Note that this equations of motion is written in terms of spatial frame.

If given differentiable manifold is actually a Lie group and if there exists a bi-invariant metric induced by the inner product on the associated Lie algebra $\mathbb{I}$, then the fully-actuated simple mechanical control system on a Lie group $\Sigma = (G, \mathbb{I}, \mathcal{F})$, the equations of motion along a trajectory $\gamma(t)$ becomes

$$\begin{aligned} \gamma'(t) &= T_e L_{\gamma(t)}(v(t)) \\ v'(t) - \mathbb{I}^{\sharp}(\mathrm{ad}^*_{v(t)} \mathbb{I}^{\flat}(v(t))) &= \mathbb{I}^{\sharp}(f(t, \gamma(t), v(t))), \end{aligned} \tag{3.2}$$

where ad is a linear map by $ad_\xi : V \to V$ by $ad_\xi \eta = [\xi, \eta]$.

3.2 Geometric tracking control on $\mathbb{R}^3$

In this section, we apply a novel error function and transport map $(\Psi, \mathcal{T})$ to the trivial case of $\mathbb{R}^3$ to understand what needs to be done for more complicated examples.

3.2.1 Error function by geodesic distance

First of all, we define a Riemannian metric to conform the requirement of 3.1. If the system trajectory can be written in a coordinate system as $\gamma t = (x^1(t), x^2(t), x^3(t)) \in \mathbb{R}^3$, and if m is the mass of the given system, define

$$\mathbb{G} := m\mathbb{G}_{\mathbb{R}^3} = \begin{bmatrix} m & & \\ & m & \\ & & m \end{bmatrix}$$

so that

$$\frac{1}{2}\mathbb{G}(\gamma(t)) \cdot (\gamma'(t), \gamma'(t)) = \text{Kinetic Energy}$$

$$\mathbb{G}^{\sharp} = \frac{1}{m} I_{3\times 3}$$

and

$$\overset{\mathbb{G}}{\Gamma}{}^k_{ij} = \frac{1}{2}\mathbb{G}^{kl}(\frac{\partial \mathbb{G}_{il}}{\partial x^i} + \frac{\partial \mathbb{G}_{jl}}{\partial x^i} - \frac{\partial \mathbb{G}_{ij}}{\partial x^l}), \qquad \text{where} \quad i,j,k,l \in \{1,2,3\}$$
$$\equiv 0 \qquad \text{since } \mathbb{G} \text{ is constant.}$$

Therefore, the equation (3.1) becomes

$$\overset{\mathbb{G}}{\nabla}_{\gamma'(t)}\gamma'(t) = \gamma''(t) = \frac{1}{m}F(\gamma(t),\gamma'(t)) \tag{3.3}$$

Next, from the result of section 2.3.1 define the geodesic distance between $q_1, q_2 \in \mathbb{R}^3$ where the geodesic connecting q_1 and q_2 is denoted by $\gamma(t)$ with $\gamma(0) = q_1$, and $\gamma(1) = q_2$:

$$\begin{aligned} d_{\mathbb{G}}(q_1,q_2) &= inf \int_0^1 \sqrt{\mathbb{G}(\gamma',\gamma')}\,\mathrm{d}t \\ &= inf \int_0^1 \sqrt{}\,\mathrm{d}t \\ &=\| \gamma(t_f) - \gamma(t_0) \|_{m\mathbb{G}_{\mathbb{R}^3}} . \end{aligned}$$

Then, we propose the natural configuration error function[4] for a fully actuated C^∞-simple mechanical control system Σ is

$$\Psi(\gamma(t),\gamma_{ref}(t)) := \frac{1}{2}\{d_{\mathbb{G}}(\cdot,,\cdot)\}^2. \tag{3.4}$$

3.2.2 Transport map by parallel transport

Differentiating 3.4 gives

$$\begin{aligned} \frac{\mathrm{d}}{\mathrm{d}t}\Psi(\gamma,\gamma_{ref}) &=< \mathrm{d}_1\Psi(\gamma,\gamma_{ref}); \frac{\mathrm{d}\gamma}{\mathrm{d}t} > + < \mathrm{d}_2\Psi(\gamma,\gamma_{ref}); \frac{\mathrm{d}\gamma_{ref}}{\mathrm{d}t} > \\ &=< \gamma(t) - \gamma_{ref}(t); \frac{\mathrm{d}\gamma}{\mathrm{d}t} > + < -\gamma(t) + \gamma_{ref}(t); \frac{\mathrm{d}\gamma_{ref}}{\mathrm{d}t} > \end{aligned}$$

$$
\begin{aligned}
&=< \gamma(t)-\gamma_{ref}(t); \frac{\mathrm{d}\gamma}{\mathrm{d}t} > + < -(I_{3\times 3})^*(\gamma(t)-\gamma_{ref}(t)); \frac{\mathrm{d}\gamma_{ref}}{\mathrm{d}t} > \qquad (3.5)\\
&=< \mathrm{d}_1\Psi(\gamma,\gamma_{ref}); \frac{\mathrm{d}\gamma}{\mathrm{d}t} > + < -(\mathcal{T})^*\mathrm{d}_1\Psi(\gamma,\gamma_{ref}); \frac{\mathrm{d}\gamma_{ref}}{\mathrm{d}t} >\\
&=< \mathrm{d}_1\Psi(\gamma,\gamma_{ref}); \frac{\mathrm{d}\gamma}{\mathrm{d}t} > + < \mathrm{d}_1\Psi(\gamma,\gamma_{ref}); -(\mathcal{T})\frac{\mathrm{d}\gamma_{ref}}{\mathrm{d}t} >\\
&=< \mathrm{d}_1\Psi(\gamma,\gamma_{ref}); \frac{\mathrm{d}\gamma}{\mathrm{d}t} - (\mathcal{T})\frac{\mathrm{d}\gamma_{ref}}{\mathrm{d}t} >\\
&=< \gamma(t)-\gamma_{ref}(t); \gamma'(t)-\gamma'_{ref}(t) >
\end{aligned}
$$

Hence, from the compatibility condition of the pair $(\Psi, \mathcal{T})$[4],

$$
\mathrm{d}_2\Psi(\cdot,\cdot) = -(\mathcal{T})^*\mathrm{d}_1\Psi(\cdot,\cdot)
$$

holds if we pick the transport map $\mathcal{T} \equiv I_{3\times 3}$, which, in turn, implies that the transport map is actually the *parallel transport* in $\mathbb{R}^3$ according to the result of section 2.3.1. Also, we make an observation that by differentiating the compatible $(\Psi, \mathcal{T})$ pair, we obtained one covector $\mathrm{d}_1\Psi(\cdot,\cdot)$ to represent a position error vector (by the sharp map) and one vector $\frac{\mathrm{d}\gamma}{\mathrm{d}t} - (\mathcal{T})\frac{\mathrm{d}\gamma_{ref}}{\mathrm{d}t}$ to represent a velocity error vector, both of which agrees with the conventional choice of errors. Later, we will use analogy to this trivial example when choosing both position and velocity error vectors for some complex systems.

3.2.3 Tracking controller

The coincidence of our choice of the square of the geodesic distance and the parallel transport along the geodesic with the configuration error and transport map, respectively, makes our geometric tracking controller be the same with normal Lyapunov based nonlinear controller for the same system. Hence, we omit the detailed design of the geometric tracking controller on $\mathbb{R}^3$.

3.3 Geometric tracking control on $SO(3)$

3.3.1 Error function by geodesic distance

Given $\Sigma = (G, \mathbb{I}, \mathcal{F})$ with $G = SO(3)$ and $\mathbb{I} = \alpha I_{3\times 3} \quad \alpha \in \mathbb{R}$, the equations of motion are

$$\begin{aligned} \dot{R}(t) &= R(t)\hat{\Omega}(t) \\ \dot{\Omega}(t) &= [\mathbb{I}]^{-1}([\mathbb{I}]\Omega(t) \times \Omega(t)) + [\mathbb{I}]^{-1} f \end{aligned}$$

From section 2.3.2, $SO(3)$ admits a bi-invariant metric and therefore the geodeisc coincides with the one parameter subgroup. Hence, the geodesic distance can be defined as follows:

$$\begin{aligned} dist(R, R_{ref}) &= \int_0^1 \sqrt{\mathbb{G}_{\mathbb{I}}(\gamma(t))(\gamma'(t), \gamma'(t))}\,\mathrm{d}t \\ &= \int_0^1 \sqrt{\mathbb{I}(T_\gamma L_{\gamma^{-1}}\gamma'(t), T_\gamma L_{\gamma^{-1}}\gamma'(t))}\,\mathrm{d}t \\ &= \int_0^1 \sqrt{\mathbb{I}(\gamma^{-1}\gamma', \gamma^{-1}\gamma')} \\ &= \int_0^1 \sqrt{\mathbb{I}(\gamma^{-1}\gamma \log(R_{ref}^T R), \gamma^{-1}\gamma \log(R_{ref}^T R))} \\ &= \int_0^1 \sqrt{\mathbb{I}(\log(R_{ref}^T R), \log(R_{ref}^T R))} \\ &= \sqrt{\mathbb{I}(\log(R_{ref}^T R), \log(R_{ref}^T R))} \\ &= \sqrt{\alpha \frac{1}{2} tr(\log(R_{ref}^T R)^T \log(R_{ref}^T R))} \\ &= \sqrt{\alpha \parallel (\log(R_{ref}^T R))^\vee \parallel_{\mathbb{R}^3}^2}. \end{aligned}$$

So we design a novel tracking error function:

$$\Psi(R, R_{ref}) = \frac{1}{2}(dist(R, R_{ref}))^2 = \frac{\alpha}{2}(\parallel \theta - \theta_{ref} \parallel)^2$$

3.3.2 Transport map by parallel transport

By differentiating the proposed tracking error function, we get

$$
\begin{aligned}
\frac{\mathrm{d}}{\mathrm{d}t}\Psi(R, R_{ref}) &=< \alpha(\log(R_{ref}^T R))^{\vee T}; \frac{\mathrm{d}}{\mathrm{d}t}(\log(R_{ref}^T R))^{\vee} > \\
&=< \alpha(\log(R_{ref}^T R))^{\vee T}; v - \mathrm{Ad}_{R_{ref}^T R}\, v_{ref} > \\
&=< ((T_e L_{R^T})^* \alpha(\log(R_{ref}^T R))^{\vee})^T; T_e L_R(v - \mathrm{Ad}_{R_{ref}^T R}\, v_{ref}) > \\
&=< \mathrm{d}_1\Psi(R, R_{ref}); R\hat{\Omega}_{e,r} >
\end{aligned}
$$

Hence we get a new error vector

$$
\mathrm{d}_1\Psi(R, R_{ref}) = \alpha(R\log(R_{ref}^T R))^{\vee})^T
$$

And a velocity error vector

$$
\begin{aligned}
\hat{\Omega}_e &= T_e L_R(v - \mathrm{Ad}_{R_{ref}^T R}\, v_{ref}) \\
&= T_e L_R(\mathrm{Ad}_e\, v - \mathrm{Ad}_{R_{ref}^T R}\, v_{ref})
\end{aligned}
$$

Observe that the velocity vector is the same with previous work while position error vector differes.[4, 10] Also, observe that htis velocity vector is not a parallel transport for the bi-invariant metric, which is disappointing, but is indeed a parallel transport for the right-Cartan map. Futher investigation on this matter is required.

3.3.3 Tracking controller

Energy function which is used for a Lyapunov candidate function is

$$
\begin{aligned}
E_{cl,r}(t) &= \Psi(R, R_{ref}) + \frac{1}{2}\mathbb{G}(R)(R\hat{\Omega}_{e,r}, R\hat{\Omega}_{e,r}) \\
&= \Psi(R, R_{ref}) + \frac{1}{2}\mathbb{I}(\hat{\Omega}_{e,r}, \hat{\Omega}_{e,r}).
\end{aligned}
$$

Then, the new geometric controller has feedforward and feedbackward terms as follows

$$
\begin{aligned}
f_{FD} &= -k_P \cdot \mathrm{d}_1\Psi(R, R_{ref}) - k_D \cdot \Omega_{e,r} \\
f_{FF} &= \mathbb{I}^\flat(\overset{so(3)}{\nabla}_\Omega(R^T R_{ref}\Omega_{ref}) + (R^T R_{ref}\Omega_{ref}) \times \Omega + R^T R_{ref}\dot{\Omega}_{ref}).
\end{aligned}
$$

We refere to the Appendix for the stability proof of this controller.

Chapter 4

Numerical Simulations

4.1 Assumptions and Simulation Environment

Numerical simulations are carried out for the case of the fully-actuated rigid body system on $SO(3)$. We choose the moment of inertia of the system to be as a $\mathbb{I}_c = I_{3\times 3}\, kg\, m^2$.

Novel geometric controller is tested alongside previously propsed [4] and [10], both of which share the same controller structure, for comparison. All controller gains for each case are set to the unit number.

General purpose numerical integrator does not preserve the special structure of $SO(3)$ and usually requires combersome post-processing at each step. Recently, Structure-preserving Lie group integrators have been actively developed using the concept of the variational integrators.[11, 3, 5] In this paper, we use a slightly modified version of the state-of-the-art Lie group integrator[9] to obtain more accurate numerical results. Program code for the new Lie group integrator is thorouly inspected and hevily tested for the integrity of result before the actual numerical simulations are carried out.

4.2 Simulation Results

We consider two cases:

(i) tracking on $SO(3)$ with

   (a) the reference trajectory with a constant angular velocity around z-axis,

   (b) the almost largest possible initial attitude error,

   (c) zero initial velocity error.

   The initial conditions of the system are

$$R(0) = exp([0; \frac{\pi}{4}; 0.99\pi]), \qquad \Omega(0) = [0; 0; 0]\, rad/sec.$$

   The reference attitude and the reference angular velocity are

$$R_{ref}(0) = I_{3\times 3}, \qquad \Omega(t) = [0; 0; \frac{2}{10}\pi]\, rad/sec.$$

(ii) tracking on $SO(3)$ with

   (a) the reference trajectory with a constant angular velocity around z-axis,

   (b) the almost largest possible initial attitude error,

   (c) very large initial velocity error in the reverse direction of the velocity of the reference trajectory.

   The initial conditions of the system are

$$R(0) = exp([0; \frac{\pi}{4}; 0.99\pi]), \qquad \Omega(0) = [0; -5; -5]\, rad/sec.$$

   The reference attitude and the reference angular velocity are

$$R_{ref}(0) = I_{3\times 3}, \qquad \Omega(t) = [0; 0; \frac{2}{10}\pi]\, rad/sec.$$

4.2.1 Large initial attitude error

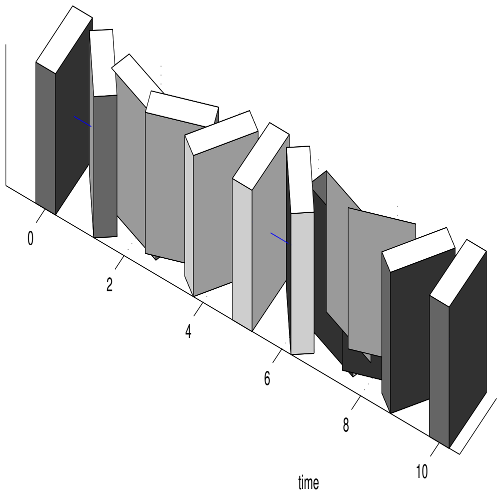

(a) Reference trajectory

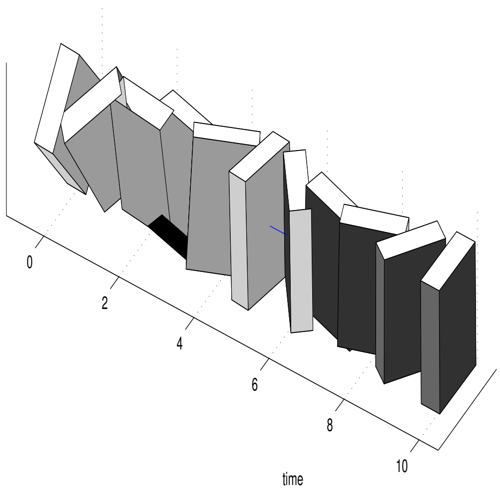

(b) Kim's trajectory

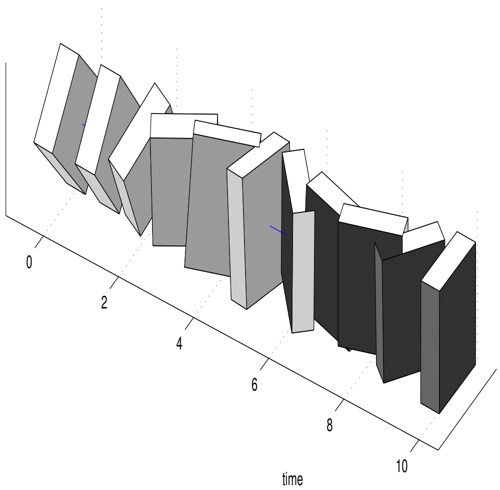

(c) Bullo's trajectory

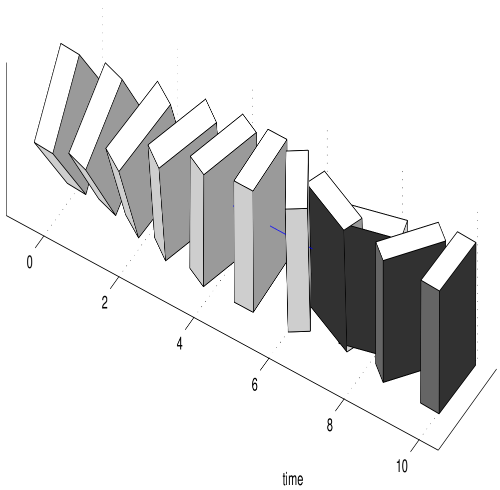

(d) Lee's trajectory

Figure 4-1: Snapshots of animiation. once per second

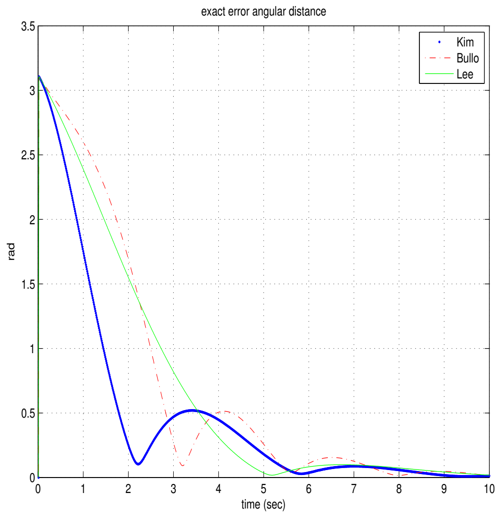

(a) exact error

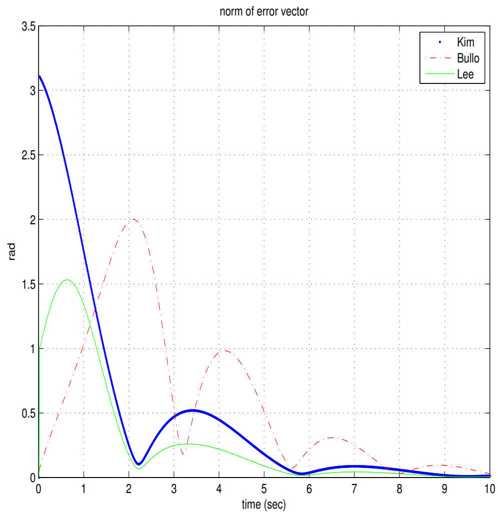

(b) measured error vector norm

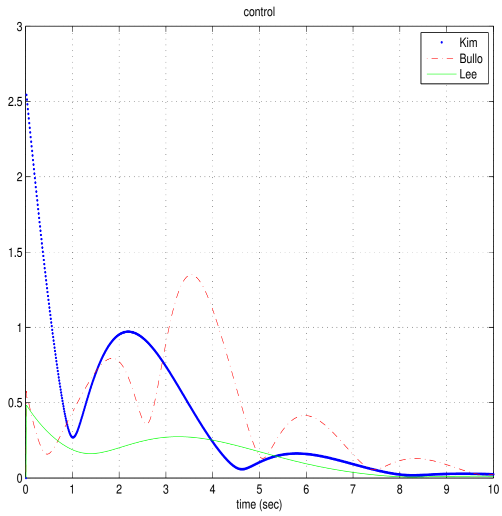

(c) control input norm

Figure 4-2:

4.2.2 Large initial attitude error with large velocity error

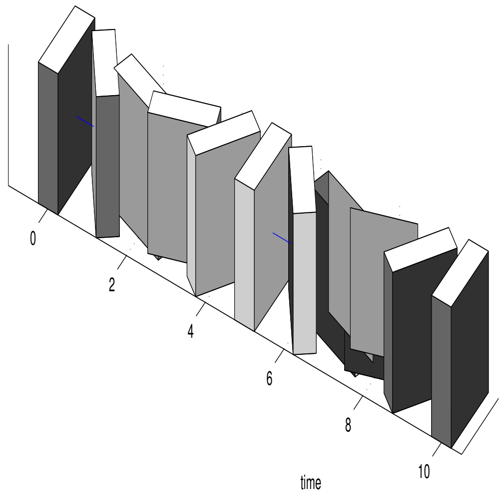

(a) Reference trajectory

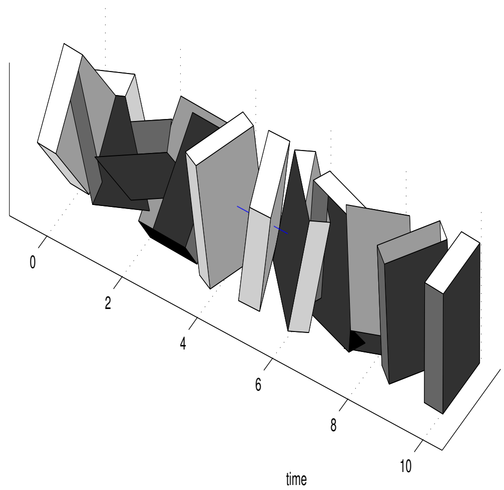

(b) Kim's trajectory

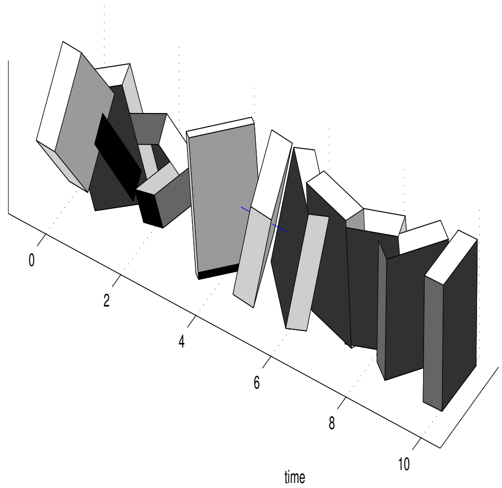

(c) Bullo's trajectory

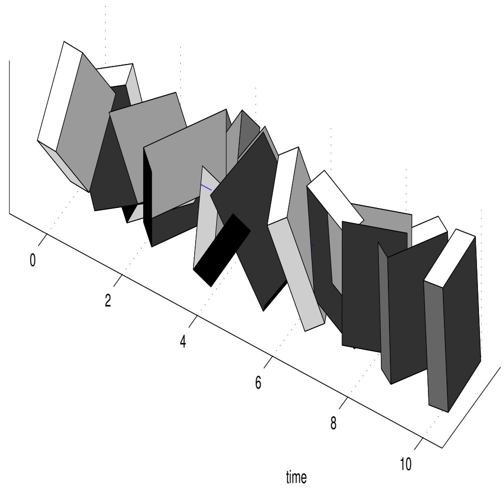

(d) Lee's trajectory

Figure 4-3: Snapshots of animiation. once per second

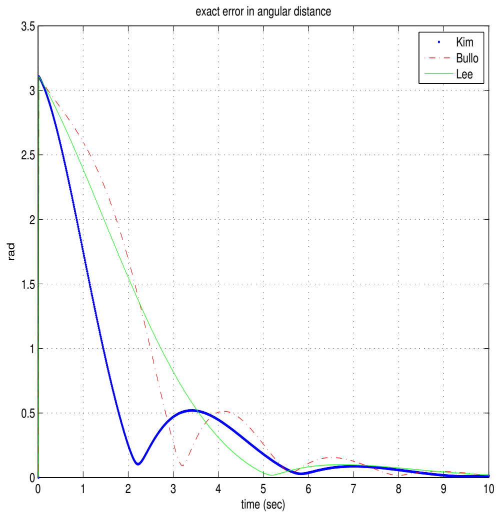

(a) exact error

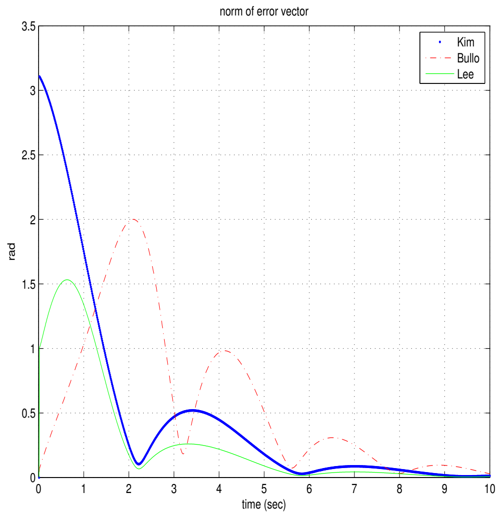

(b) measured error vector norm

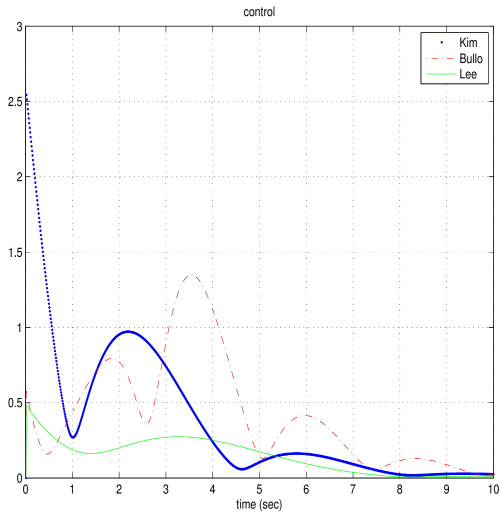

(c) control input norm

Figure 4-4:

Chapter 5

Conclusion

In this thesis, we proposed a novel pair of the configuration error and transport map, which are the pair of the square of the geodesic distance and the parallal transport. Our configuration error function is proved to be a Morse Function.[13] From this choice, a new position error vector on $SO(3)$ is found. The norm of this position error vector is, by design, exactly proportional to the actual angular error measured by the instantaneous screw motion connecting current attitude and current reference attitude. The geometric controller based on our configuration error and transport map is shown to be almost globally exponentially stable as well as to be able to track reference trajectory almost globally asymtotically.

Numerical simulation is carried out by the state-of-the-art Lie group integrator. Our controller estimated configuration error exactly while others' [**?**, 4] were nearly proportional or even inversely proportional in some range. Therefore, our controller showed the fastest response while the error between the staten and the reference is relatively large. Interestingly enough, however, the settling time of the three compared controller is very similar. Hence, further investigation on the convergence rate is required. Also, we observed that all the compared controllers exert force in the opposite direction of the desired control direction at some points. The time stamps of this strange behavior is almost identical among the controllers considered. Intuitively, this phenomenon tells that our estimate of velocity error vector is wrong somehow because all the three controllers differ by the choice of configuration functions and their position error vector but at, the same time, share the exactly same velocity error vector. This also needs to be added to the long list of future work.

Our controller is based on the existence of the geodesic distance and in turn the existence of bi-invariant metric. Some Lie groups, such as Special Euclidean Group or $SE(3)$, does not have this property. Hence, extention to the current result is necessary.

Bibliography

[1] A. M. Bloch, J. Baillieul, P. Crouch, and J. Marsden. *Nonholonomic Mecanics and Control*, volume 24 of *Interdisciplinary Applied Mathematics*. Springer, November 2004.

[2] William M. Boothby. *An Introduction to Differentiable Manifolds and Riemannian Geometry*. Academic Press, San Diego, California, revised second edition, 2003.

[3] Nawaf Bou-Rabee and Jerrold E. Marsden. Hamilton-pontryagin integrators on lie groups part I: Introduction and structure-preserving properties. *Journal of the Society for the Foundations of Computational Mathematics*, 9:197–219, 2009.

[4] Francesco Bullo and Andrew D. Lewis. *Geometric Control of Mechanical Systems*, volume 49 of *Texts in Applied Mathematics*. Springer, Houston, Texas, 2005.

[5] Elena Celledoni, Håkon Marthinsen, and Brynjulf Owren. An introduction to lie group integrators - basics, new developments and applications. *Journal of Computationl Physics*, 2013.

[6] Manfredo P. do Carmo. *Differential Geometry of Curves and Surfaces*. Prentie-Hall, Inc., New Jersey, 1976.

[7] Emilio Frazzoli. *Robust Hybrid Control for Autonomous Vehicle Motion*. PhD thesis, Massachusetts Institute of Technology, June 2001.

[8] Sigurdur Helgason. *Differential Geometry, Lie Groups, and Symmetric Spaces*, volume 80 of *Pure and Applied Mathematics*. Academic Press, New York, 1978.

[9] Marin Kobilarov, Keenan Crane, and Mathieu Desbrun. Lie group integrators for animation and control of vehicles. *ACM Transactions on Graphics*, 28(2):16:1–16:14, April 1009.

[10] Taeyoung Lee. Geometric tracking control of the attitude dynamics of a rigid body on SO(3). *American Control Conference*, pages 1200–1205, June-July 2011.

[11] Taeyoung Lee, N. Harris McClamroch, and Melvin Leok. A lie group variational integrator for the attitude dynamics of a rigid body with applications to the 3d

pendulum. *Proceedings of the 2005 IEEE Conference on Control Applications*, pages 962–967, August 2005.

[12] Daniel Mellinger and Vijay Kumar. Minimum snap trajectory generation and control for quadrotors. *2011 IEEE International Conference on Robotics and Automation*, May 2011.

[13] Marston Morse. The existence of polar non-degenerate functions on differentiable manifolds. *Annals of Mathematics*, 71(2):352–383, March 1960.

[14] Frank W. Warner. *Foundations of Differentiable Manifolds and Lie Groups*, volume 94 of *Graduate texts in mathematics*. Springer-Verlag, New York, second edition, 1983.